Hybrid Simulation of Scattering Distribution in Cone Beam CT

Raphaël Thierry, Alice Miceli, Jürgen Hofmann

Laboratory for Electronics/Metrology/Computed Tomography, EMPA
8600-Dübendorf, Switzerland; Phone: +44 1 823 40 89, Fax +44 1 823 45 79;
raphael.thierry@empa.ch, alice.miceli@empa.ch, juergen.hofmann@empa.ch

Abstract
This paper presents a hybrid simulator for the fast calculation of x-ray projections. Uncollided radiations are determined with a ray-driven method whereas the scattering signal is partitioned into single and multiple scattering, respectively estimated with an accelerated deterministic method and a coarse Monte Carlo simulation. The simulator takes into account the full acquisition chain, from the emission of a polyenergetic beam of photons, their interactions with the scanned object until their energy deposit in the detector. Object phantoms can be spatially described in form of voxels, mathematical volume primitives or CAD models. The hybrid method has been validated with the Monte Carlo code Geant4 on aluminium phantoms with varying size and object-to-detector distance. Good agreement has been found between the two methods. The acceleration achieved by the hybrid method on a single projection lies between two to four orders of magnitude. The proposed simulator has been developed for industrial cone-beam CT scanners and the correction of scatter artefacts.
Keywords : Computed Tomography, Monte Carlo, Hybrid Simulation, Scattering, Forced Detection

1. Introduction

Scattered photons and beam hardening are the dominant effects that lead to significant degradation of the image quality in Cone-beam CT systems. Both effects contribute to strong cupping artefacts and cause streaks to appear between dense objects in the reconstructed image [1]. Moreover, additional scattering with the environment (wall, shieldings, etc) further limits the contrast [2].
The amount of scattering in X-ray computed tomography is a multivariate function, where the geometry of the setup, the polyenergetic beam distribution and the nature of the object (material, thickness and geometry) play a key role [3, 4]. Often, the scatter is measured with regard to the primary photons and the referred quantity is called the scatter-to-primary ratio (SPR). As the SPR is an increasing function of the object thickness, field size and atomic number Z [3, 5], the scanned objects encountered in industrial X-ray CT (such as cast-parts of the automotive and aeronautics fields) generate images with high SPR.
Methods to reduce the scatter can virtually be splitted into hardware and software techniques. Methods relying on hardware-modifications of the CT measurement chain (beams stops, filtering, collimators, etc) have proved their efficiency on specific applications; yet these methods often require mechanical modifications of the equipment which extend the scanning time and the resulting scatter reductions are often suboptimal.
With the steady progress in computation capabilities, elaborated software techniques have become the leading edge in scattering reduction techniques. Recent publications showed that they provide the most accurate and advantageous solution [6, 7]. They rely on MC computer simulations, numerical approximations of the scattering functions, or by combining the two in so-called hybrid methods. Some authors adapted MC simulators with the possibility to handle the geometric complexity with CAD models

[8], or developed accelerated in-house MC with techniques such as the Forced Detection (FD) [9]. Because single scattering (i.e photons undergoing solely one interaction with the object) often constitutes the prevailing part of the scattering signal, deterministic methods have alternatively been proposed to assess the scattering in radiographic images [5]. They present the advantage to provide a noise-free scattering estimation. Yet they still require a significant acceleration for their use in CT image correction, and only apply to objects generating predominantly single scattering, which excludes large objects made of dense materials. Hybrid methods [6, 10] take advantage of the complementarities between deterministic and stochastic methods. Hence, they represent potential tools in scattering corrective methods and CT post-processing chain without leading to prohibitive increase of the overall processing time.
This paper describes a new hybrid method, where an acceleration of the deterministic simulation of the single scattering is presented and the estimation of the multiple scattering is addressed with a coarse MC on a primitive shaped-object. We illustrate the accuracy and acceleration factors achieved by the method in various simulation settings.

2. Methods

2.1 Accelerated deterministic simulation of single scattering

The deterministic model presented here uses the form factor (FF) and the incoherent scattering function (ISF) approximations, respectively for Rayleigh and Compton scattering of unpolarized photons. The FF and ISF values, as well as the mass attenuation coefficients are taken from the NIST and EPDL97 database, distributed in [11]. The deterministic single scattering simulation corresponds to a numerical evaluation of the integral over the volume defined by the active voxels (i.e voxels having a strictly positive value) and the energy spectrum of the x-ray tube. The integral is carried out for each detector element with index (l,m), and it can be expressed as :

$$I_s^1(l,m) = \iint_{v \in V, E} \varepsilon_{\text{det}}(E,\theta,Z_{\text{det}}).dN_V(E).(dp_{Ra}(E) + dp_{Co}(E))dEdv \qquad (1)$$

where $\varepsilon_{\text{det}}(E,\theta,Z_{\text{det}})$ models the detector response as a function of the energy E, the angle θ between the photon and the normal vector of the detector pixel, and Z_{det} the atomic number of the detector. The quantity $dN_V(E)$ represents the number of photons emitted by the source S at energy E an reaching the voxel V, $dp_{Ra}(E)$ and $dp_{Co}(E)$ represent the probability of a photon to undergo a scattering in V, respectively by Rayleigh and by Compton scattering, and reaching the detector element (l,m). The attenuation factor, which is included in the terms $dN_V(E)$, $dp_{Ra}(E)$ and $dp_{Co}(E)$, is computed analytically with an incremental Siddon algorithm. More detailed expression of the different terms can be found in [5, 6].
The time needed to calculate the scattering signal I_s^1 depends on the number of active voxels, the number of detector pixels N_{det}, and to a less extent to the number of energy bins used to sample the x-ray spectrum. In cone-beam geometry N_{det} can be relatively high therefore calculating (1) for each individual pixel would increase the computing

time prohibitively. An effective way to reduce the computing time consists in "forcing" the photons to interact only with a subset of the N_{det} pixels. The method called Forced Detection (FD) is originally a variance reduction technique used to speed up the MC calculations. It takes advantage of the relative smoothness of the signal produced by the single scattering. For each voxel V, a number N_{FD} ($N_{FD} << N_{\text{det}}$) indexes are chosen randomly, and a weighting factor $w = N_{\text{det}} / N_{FD}$ is assigned to correct for the fact that only the "forced" pixels of the detector have been touched. The scattering estimations produced with the FD method are no longer noise-free, yet they can benefit largely from de-noising methods, for instance with the Richardson-Lucy (RL) algorithm [9]. The RL is mathematically equivalent to the Maximum-Likelihood Expectation Maximization (ML-EM) and so inherit from the same properties, i.e. robustness to noise, ability to cope with truncated data and an inherent positivity constraint. We associate the FD accelerated deterministic method with the RL de-noising, and we refer in the rest of the paper to the "FD+RL" method.

2.2 Monte Carlo simulation of multiple scattering

Because usual methods such as build-up factors, scaling [12] or convolutions [13] of single scattering can not fully account for multiple scattering, we propose to use a MC method instead. We propose to build a virtual object with the volume primitives available in the MC code Geant4. In order to produce a similar multiple scattering signal, the object keeps key characteristics of the scanned object: material composition, volume, center of gravity and an identical path-length histogram[1]. We will refer in the rest of the paper to the Equivalent Path-Length Object (EPLO). The aim is to estimate the multiple scattering of the object, I_s^m, as a function of the (previously calculated) single scattering I_s^1, and from $I_{s,E}^m$ and $I_{s,E}^1$, respectively the first and multiple scattering of the EPLO. The characteristic of the EPLO is expected to guaranty that :

- the multiple scattering $I_{s,E}^m$ integrated over the full area of the detector is near to the one produced by the object, hence we note κ the scalar such as

$$\kappa = \sum_{l,m} I_{s,E}^m(l,m) \approx \sum_{l,m} I_s^m(l,m) \qquad (2)$$

- the ratio r_E between the multiple and single scattering of the EPLO is near to the one produced by the object. This assertion attempts to model the phenomenon of spreading and smoothing observed between the image of the single scattering and the one of the multiple scattering. Practically, $I_{s,E}^m$ and $I_{s,E}^1$ are first de-noised, and the point clouds $\left(I_{s,E}^1(l,m), r_E(l,m) = I_{s,E}^m(l,m) / I_{s,E}^1(l,m)\right)_{l,m}$ are later fitted with a polynomial P_E. Finally we can re-express r_E as an estimator of the ratio between the multiple and single scattering of the real object:

[1] the histogram of crossed lengths produced by the scanned object is easily obtained through the ray-tracing process used to generate the primary (unscattered) photons.

$$r_E \approx P_E\left(I^1_{s,E}\right) \approx \frac{I^m_s}{I^1_s} \quad (3)$$

- Finally we express that $I^m_s(l,m)$ is the product of $I^1_s(l,m)$ by the ratio $r_E(l,m)$. The multiple scattering is finally obtained after operating a cubic interpolation smoothing of $I^m_s(l,m)$, noted S, so as to erase the possible high frequencies present in $I^1_s(l,m)$. Finally the multiple scattering is expressed by :

$$I^m_s = \frac{\kappa}{\sum_{l,m} S\left(I^1_s(l,m).r_E(l,m)\right)} S\left[I^1_s.r_E\right] \quad (4)$$

3. Materials and Evaluations

3.1 Phantoms

Three software phantoms in aluminium were studied: (A) a parallelepiped of dimension 10 cm x 10 cm x 2 cm, (B) a step-wedge with steps of 2, 4, 6, 8 and 10 cm, and (C) a pilling up of centred cylinders with external radius of 2, 3, 4, 5, 6, 8, 10 and 11 cm, and an internal radius of 1 cm. Figures and parameters are illustrated in figure 1.

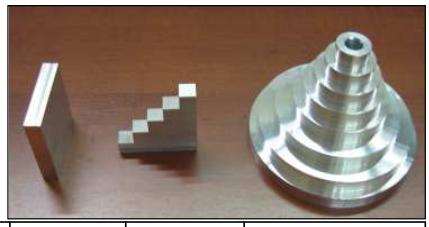

		Parameters	Object A	Object B	Object C
		Volume (cm³) :	200	120	2306
Simulated Radiation	Primary	Object Grid : Voxel size (mm³) : Detector Grid : Pixel size (mm²) :	512x512x512 0.19x0.19x0.19 512x512 0.058x0.058	512x512x102 0.19x0.19x0.19 512x512 0.058x0.058	768x768x558 0.28x0.28x0.28 512x512 0.084x0.084
	Scattering	Object Grid : Voxel size (mm³) : Detector Grid : Pixel size (mm²) :	128x128x128 0.78x0.78x0.78 150x150 0.2x0.2	128x128x128 0.78x0.78x0.78 150x150 0.2x0.2	128x128x93 1.71x1.71x1.71 216x216 0.2x0.2
		D_{SO} : Distance Source-Object (mm):	1000	1000 / 1380	1000/ 1320

Figure 1: Phantoms and associated parameters

3.2 Geometric settings and simulation parameters

The simulations performed in this paper are intended to model an industrial cone-beam CT scanner. The CT device is equipped with a large flat CsI scintillator and a charge-coupled device (CCD). Focal lengths varied between 1000 and 1380 mm, the distance from the source to the detector is set to 1500 mm, and detector sizes used were 300 x 300 mm^2 and 432 x 432 mm^2 for the object C. For the simulation purpose we used a point isotropic monoenergetic source of photons of 250 keV and a full detector efficiency, i.e. $\varepsilon_{\text{det}}\left(E,\theta,Z_{\text{det}}\right) = E$. MC simulations of objects and the EPLOs were

performed with respectively 2.10^9 and 10^8 photons. The RL fitting was performed over 20 iterations with a Gaussian of variance σ=10, a window size of 16x16 pixels. The determination of the multiple scattering used a polynomial P_E of order 5 and a cubic smoothing spline with the smoothing parameter p set to 0.05.
We analysed the single scattering image by comparing the conventional MC method and the accelerated deterministic method on the phantom A placed at 1000 mm from the source. We refer to the subscript "FD+RL" for the method using the Forced Detection followed by RL fitting. The parameter used to assess the precision of each simulation was the Root Mean Square Error (RMSE) overall the detector surface where the reference intensity corresponds to a full deterministic calculation, i.e. by calculating the equation (1) for all the elements (l,m) of the pixelised detectors.

4. Results

4.1 Estimation of the single scattering

We simulated a projection of object A placed at 1000 mm from the focal source. Projections simulated with the MC method used 10^7, 10^8 and 10^9 photon histories and were de-noised with the RL fitting. Besides we analysed the FD+RL method with number N_{fd} varying between 1 and 500. The figure 2 illustrates the results in term of reconstruction time versus RMSE. We observe that the FD+RL give satisfactory results from a few number of Forced Detection. Hence, N_{fd} =5 results in a RMSE comparable to the MC simulation with 10^9 photon and requires four order of magnitude less computing time. The robustness to noise of the FD+RL is to put together with the characteristics of the maximum-likelihood expectation-maximization algorithm, and the method applies well to the deterministic approach, although the underlying statistical distribution is no longer poissonian.

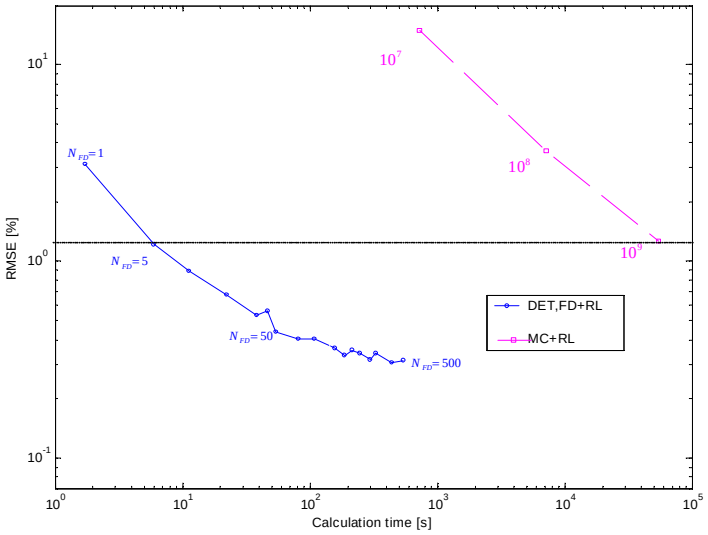

Figure 2 : Computation time versus Residual Mean Squared Error

Increasing the number of FD contributes to decrease the RMSE, nevertheless the gain becomes poor with regard to the additional calculation time. The MC simulation with 10^9 photon histories took 908 minutes on a PC with a 2 GHz microprocessor, when the FD+RL with N_{fd} =10 needs only a tens of seconds.

4.2 Estimation of multiple scattering

Multiple scattering was estimated according to the procedure described in section 2.C. The quantitative accuracy of the multiple scattering is estimated via the ratio (expressed in percent)

$$R = 100 \frac{\phi}{\phi_E} \frac{\sum_{i,j} I^m_{s,E}(i,j)}{\sum_{i,j} I^m_s(i,j)} \tag{6}$$

where ϕ and ϕ_E represent the photons histories used respectively for simulation of the object and its EPLO. Ratios r_1 and r_2 representing the relative contribution of the single and double scattering were also calculated. The ratio R was calculated using the full area of the detector, whereas r_1 and r_2 were calculated in a rectangular window W selected in the penumbra of the object (white frame in thumbnails in figure 3). An illustration of the horizontal and vertical profile of the SPR is also given for object B and C (figure 3). Table 1 lists the different ratios for the different settings.

Table 1 : Ratios obtained in the different configurations

Phantom	A		B		C	
Volume (cm^3)	200		120		2306	
D_{SO} : Distance source object (mm)	1000	1380	1000	1380	1000	1320
Mean path-length (mm)	19.9	20.3	56.6	55.6	108.3	110.7
R	99.0	98.0	99.0	96.0	108.0	103.0
$r_1 = 100.\sum_W I^1_s / \sum_W I_s$	89.6	84.2	90.6	82.1	71.2	62.7
$r_2 = 100.\sum_W I^2_s / \sum_W I_s$	7.7	11.5	7.2	13.3	16.2	19.9
$r_{1+2} = 100.\sum_W (I^1_s + I^2_s) / \sum_W I_s$	97.3	95.7	97.8	95.4	87.5	83.0
$SPR = 100.\sum_W I_s / \sum_W I_p$	1.8	7.9	0.9	4.0	6.3	15.4

The ratio R ranges from 96 to 108 %. The multiple scattering of object A is well quantified which is not surprising since the geometry of the EPLO is close to the one of the object. The object B at a distance source-object (D_{SO}) of 1380 mm and the object C at D_{SO}= 1000 mm present the largest bias. From the results in table 1 we observe that:

- ratio r_1 decreases with D_{SO} which is in agreement with previous studies [3, 5].
- ratio r_2 increases with D_{SO}, and so does also the multiple scattering ($r_1 + r_m = 1$)
- the single scatter is usually dominant over multiple scatter for our studied cases. More precisely the ratio r_{1+2} covers more than 83 % of the scattering amount.

- the scatter-to-primary ratio (SPR) is found to increase with the object's field size, the mean path-length and D_{SO}, which is in agreement with past studies [3, 4].

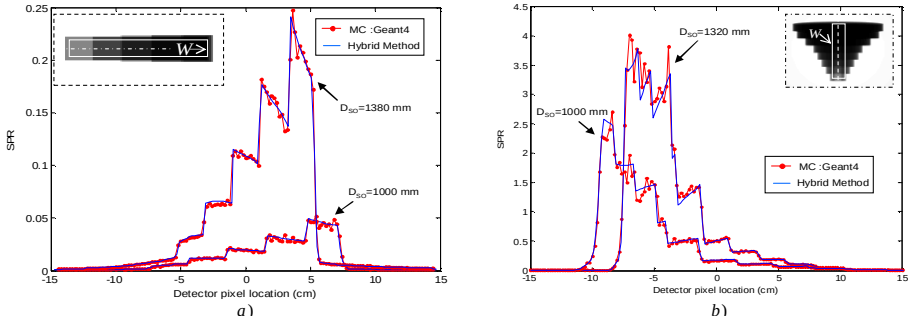

Figure 3 : Profile of scatter-to-primary ratio. (a), the SPR of the object B along the central horizontal detector line, and in (b) the SPR of the object C along the central vertical detector column

The profiles in figure 3 let guess the outlines of the different steps of the objects which underlines the relation between the SPR and the crossed path-length. For the object C the SPR is maximal behind 20 cm of aluminium where it surpasses 350 %. In comparison, the SPR of object B is maximal behind the 10 cm of aluminium and hardly reaches 25 %. After 10 cm, the SPR of object C is around 0.5, so twice as important as in B for the same thickness. This underlines the combined effect of the object's volume and crossed-thickness onto the SPR.

4.3 Comparison with Geant4

Images generated by the Hybrid simulation method are compared with those obtained with Geant4 on objects B (figure 4) and C (figure 5) and lead to the following comments:

1. In all cases, the Hybrid method is in excellent accordance with the MC results; the multiple scattering is quantitatively in good agreement (between 96 and 108% of the real energy deposit), and the form is well retrieved for short object-to-detector distance; for larger distances, the form of multiple scattering can not longer be assessed on the basis of the single scattering form and errors appear. Local errors that may occur are nevertheless largely damped by the distance effect that lowers the relative importance of multiple scattering.
2. Both single and multiple scatter results obtained with the hybrid approach present considerably reduced statistical fluctuations, which make it a good candidate for scattering correction of CT image reconstruction.
3. Since the single scattering dominates the total scattering intensity, it is prone to share its maximum with the SPR. The maximum is obtained where a compromise between the thickness of scattering matter and the attenuation factor is achieved; both for B and C this spot is located behind the smallest step thickness, so after the 20 mm step.
4. Single and multiple scatter distributions have similarities, yet they are distinct in some points : shapes can be different and scatter peaks for single and multiple scatters do not coincide with each other. For small D_{SO}, the outline of the object vanish partially (figure 5-c) or even completely (figure 4-c).

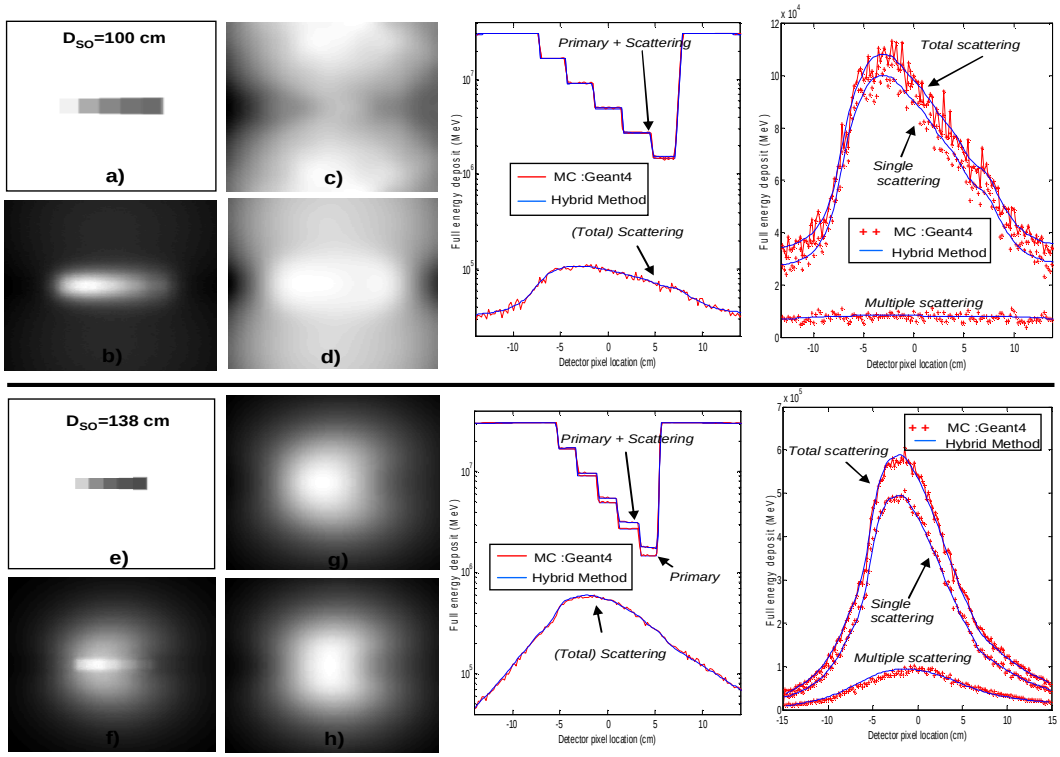

Figure 4 : Projection of object B at D_{SO}=100 cm (above the bold line) and at D_{SO}=138 cm (below the line). Details of primary (a,e), single scattering (b,f), multiple scattering respectively obtained with Geant4 (c,g) and with the hybrid method (d,h). Profile along the central horizontal line is plotted. detail of the decomposition of the scattering into single and multiple scattering is also shown.

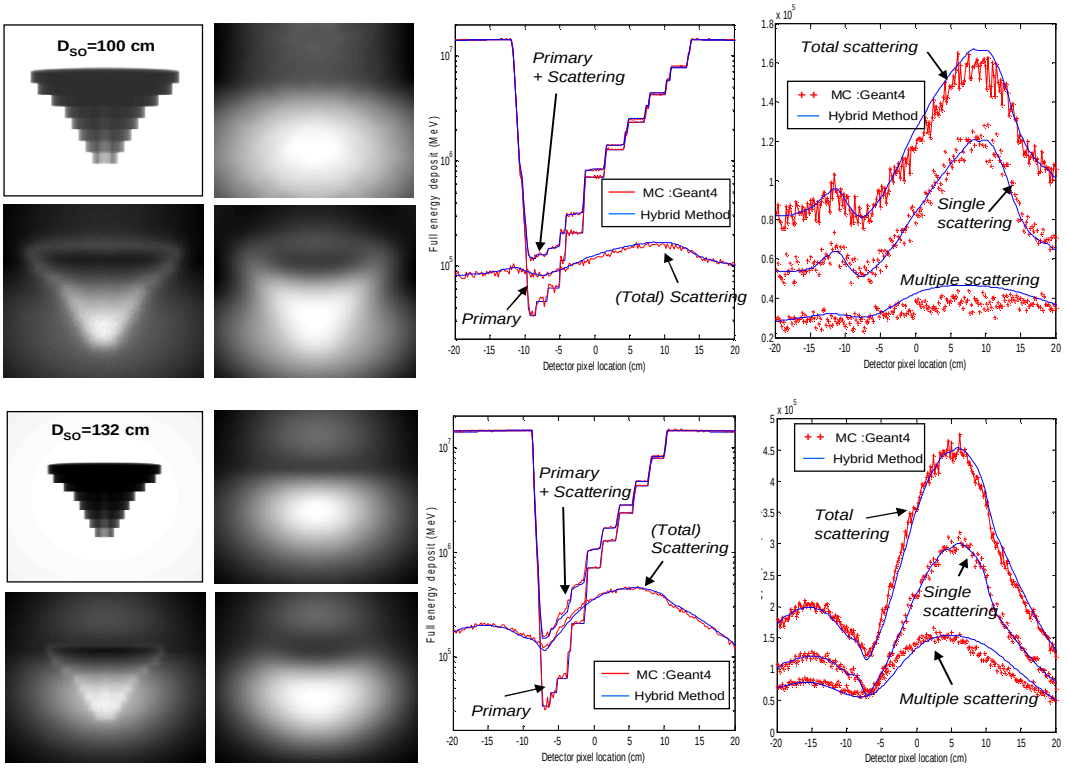

Figure 5: Same illustrations as in figure 4 with object C at D_{SO}=100 cm and at D_{SO}=132 cm. Profiles are shown along the central vertical line

5. Conclusion

An hybrid method for the rapid estimation of single and multiple-scatter intensity in cone-beam x-ray CT has been presented and validated on simulated data with the Monte Carlo (MC) code Geant4. Both methods were compared on radiographic images obtained from phantoms having various volume, forms, and distance to the detector and all results were in excellent agreement. The accelerated deterministic approach (FD+RL) produces a fast estimation of single scattering with high accuracy. The speed-up achieved by using the FD+RL over standard methods (MC or deterministic) depends on the volume of the object. In our study we have found the acceleration to vary between two to four orders of magnitude. On a single PC, the FD+RL method enabled to simulate the single scattering in ten of seconds and up to ten minutes for the biggest object.

In our proposed model, the multiple scattering was estimated by mean of a coarse MC on an virtual object having common features with the object under study. The results showed a good quantification of the multiple scattering, with deviations of less than 8%. These errors appear fairly acceptable with regard to the relative small contribution of multiple scattering - between 10 and 38% of the total scattering intensity.

In particular this study pointed out the geometrical effect played by the distance to the detector and the size of the object on the contribution of the n-fold scatter intensities. The results obtained revealed the difficulty to find an estimator of the multiple scattering on the basis of the single scattering signal. We found that for short distance to the detector, our method is quite accurate; for longer distances, errors are damped by the relatively small importance of multiple scattering.

In summary, the developed simulator enables a rapid calculation of an accurate noise-free scattering intensity. Therefore the simulator can be dedicated for the scattering correction in x-ray CT. Future work will focus on the validation of the presented hybrid simulator on experimental data.

References

1. P. Joseph and R. Spital " The effects of scatter in X-ray computed tomography", Med. Phys., vol 9, no 2, pp 464-47, 1982.
2. A. Miceli, R. Thierry, A. Flisch, U. Sennhauser, F.Casali, "Monte Carlo simulations of a high resolution X-ray CT system", *NIM- A (correction status), 2007*
3. Kalender W A "MC Calculations of x-ray data for diagnostic radiology" *Phys. Med. Biol.* **26** 835–49, 1981
4. Johns P C and Yaffe M "Scattered radiation in fan beam imaging systems" *Med. Phys.* **9** 231–9, 1982
5. N. Freud. *Modélisation et simulation de systèmes d'imagerie par rayons X ou gamma* PhD Thesis : Institut National des Sciences Appliquées de Lyon, 2003
6. Y. Kyriakou, Thomas Riedel and Willi A Kalender "Combining deterministic and Monte Carlo calculations for fast estimation of scatter intensities", Phys. Med. Biol. 51, 4567-4586, 2006
7. W Zbijewski and F. Beekman "Efficient MC Based Scatter Artifact Reduction in Cone Beam Micro-CT ", IEEE Trans. Med. Imag. , vol 25, no 7, july 2006

8. Gerd-Rüdiger Jaenisch et al “McRay – A Monte Carlo Model Coupled to CAD for Radiation Techniques”, ECNDT 2006, Tu.4.3.3
9. A.P. Colijn and F.J. Beekman “Accelerated Simulation of Cone Beam X-Ray Scatter Projections”, IEEE Transactions on Medical Imaging, vol 23, no 5, 2004.
10. N. Freud, J.-M. Létang and D. Babot A hybrid approach to simulate multiple photon scattering in X-ray imaging *NIM-B, vol 227, n° 4, 551-558, 2005*
11. D.E. Cullen, J.H. Hubbell, L. Kissel, EPDL97: the evaluated photon data library, ’97 version, Tech. Rep. UCRL-ID-50400, Vol. 6, Rev. 5, LLNL, 36 p, 1997
12. Werling A, Bublitz O, Doll J, Adam L E and Brix G “Fast implementation of the single scatter simulation algorithm and its use in iterative image reconstruction of PET data” *Phys. Med. Biol.* **47** 2947–60, 2002
13. Goggin A S and Ollinger J M “A model for multiple scatter in fully 3D PET” *Proc. IEEE Nucl. Sci. Symp. Med. Imaging Conf.* vol 4, pp 1609–13, 1994